Title of Publication *Edited by*
TMS (The Minerals, Metals & Materials Society), Year

MODELING OF THE COUPLED MOTION OF RIGID BODIES IN LIQUID METAL

Michael Barkhudarov[1], Gengsheng Wei[1]

[1]Flow Science, Inc.; 683A Harkle Road; Santa Fe, New Mexico, 87505, USA

Keywords: Computational fluid dynamics; Fixed-mesh method; Moving solid objects; Casting

Abstract

Casting processes often involve moving solid bodies that control the flow of metal, such as ladles and stoppers in gravity casting, shot pistons in pressure die casting and die components in squeeze casting. Simulation of these processes requires modeling the motion of the liquid metal, the solid bodies and the interaction between them. The present work describes a control-volume based model for general moving objects in fluids. Three-dimensional solid objects are modeled as rigid bodies moving through fixed rectangular grids. The location of the objects in the grid is described with fractional area and volume coefficients. New area and volume fractions are calculated at each time step using the updated object locations and orientations. The motion of each object can be either prescribed or dynamically coupled with fluid flow. For coupled motion, the motions of rigid bodies are governed by fluid, gravitational and control forces and torques. The action of a moving object on the fluid is modeled by introducing appropriate volumetric sources and sinks in each control volume that contains a moving surface. Tangential velocity of the moving object surface is also introduced into the shear stress terms of the momentum equations for the fluid. After validating the model against experimental data for drop tests of heavy simple-shaped objects in water, an example of liquid metal pouring simulation is also shown.

Introduction

There are many engineering practices in which solid objects move in fluid. Conventional CFD methods for moving objects are mainly based on moving and deforming mesh techniques [1, 2]. Usually these methods do not allow the distance between moving objects to be too small and they also fail when the distortion of the mesh becomes severe, limiting the complexity and generality of the motion. Although re-meshing may help overcome these problems, it requires repeated mesh generation in the computation and, therefore, can be computationally expensive.

The present work utilizes the Fractional Area-Volume Obstacle Representation (FAVOR^{TM}) technique to describe the object geometry in fixed rectangular meshes by means of area fractions (A_f) and volume fractions (V_f) [3]. In each computational control volume, V_f is defined as the ratio of the volume open to fluid to the total cell volume, and A_f is defined at each of the six faces as the ratio of the respective open area to the total area. A fixed-mesh method for general moving objects (GMO) based on the FAVOR^{TM} technique has been developed to model fully-coupled motion of solid bodies in fluids [4, 5]. At each time step, A_f and V_f are updated in accordance with the object's motion. Multiple moving objects can exist in the same domain and each of them can have a different type of six-degrees-of-freedom (DOF), fixed-point or fixed-axis motion, either prescribed or dynamically coupled with fluid flow. This fixed-mesh GMO method has advantages over the moving and deforming mesh methods because it treats complex moving objects very efficiently and conveniently. The motion of each moving object is not restricted in

its complexity. A physically acceptable treatment of collisions between objects is also possible. Potential applications of the GMO method exist not only in casting, but in many other engineering problems.

Mathematical Model

General motion of a rigid body can be divided into a translation along with a reference point and a rotation. For six-DOF motion, it is convenient to select the object mass center as the reference point. Equations of motion governing the two separate motions are [6]

$$\vec{F} = m\frac{d\vec{U}_G}{dt} \tag{1}$$

$$\vec{T}_G = [J]\cdot\frac{d\vec{\omega}}{dt} + \vec{\omega}\times([J]\cdot\vec{\omega}), \tag{2}$$

where $\vec{F}$ is the total force, m is the mass of the moving object, $\vec{T}_G$ is the total torque about the mass center in a body-fixed reference system ("body system"), $\vec{U}_G$ is the mass center velocity, $\vec{\omega}$ is the angular velocity, and [J] is the moment of inertia tensor about the mass center. Equation (1) is solved in an inertial reference system, while Eq. (2) is solved in a body-fixed system. The body-fixed coordinate system has its origin at the mass center, and its coordinate axes are initially parallel to those of the space system. A coordinate transformation between the space and body systems is done using a coordinate transformation tensor [R] satisfying

$$\frac{d[R]}{dt} = [\Omega]\cdot[R] \tag{3}$$

where [Ω] is the cross-product matrix of the object's angular velocity. The continuity equation, with the area and volume fraction factors included, is

$$\frac{V_f}{\rho}\frac{\partial\rho}{\partial t} + \frac{1}{\rho}\nabla\cdot(\rho\vec{u}A_f) = -\frac{\partial V_f}{\partial t} \tag{4}$$

where ρ is the fluid density, $\vec{u}$ fluid velocity, V_f volume fraction, A_f area fraction. A key modification of Eq. (4) is that in its discretized form the right-hand side is replaced with

$$-\frac{\partial V_f}{\partial t} = \vec{U}_{obj}\cdot\vec{n}\,S_{obj}\big/V_{cell} \tag{5}$$

where S_{obj}, $\vec{n}$ and $\vec{U}_{obj}$ are surface area, surface normal vector and velocity of moving object boundary in a mesh cell, respectively, and V_{cell} is the cell total volume. The term on the right-hand side of Equation (5) gives better accuracy than its equivalent on the left-hand side when tracking the moving interface as it passes from one control volume to another. The derivation shows that no additional terms exist in the momentum equations if they are written in a non-conservative form

$$\frac{\partial\vec{u}}{\partial t} + \frac{1}{V_f}\left(\vec{u}A_f\cdot\nabla\vec{u}\right) = -\frac{1}{\rho}\left[\nabla p + \nabla\cdot(\tau A_f)\right] + \vec{G} \tag{6}$$

Here p is pressure, τ is the viscous stress tensor and $\vec{G}$ is gravity. The only modification of the momentum Eq. (6) is the addition of the tangential velocity of the moving object boundaries in the wall shear stress terms.

The volume-of-fluid, VOF, method is used to track fluid free surfaces in the fixed grid [8]. The fluid fraction function, F, is defined as equal to one inside the fluid, and to zero otherwise. Averaged over a control volume containing free surface, the value of the fluid fraction falls into the range between zero and one, and, in general, will vary in time and space as the fluid moves through the computational domain. The kinematic transport equation for the VOF function is

$$\frac{\partial F}{\partial t} + \frac{1}{V_f} \nabla \cdot (F \vec{u} A_f) = 0 \tag{7}$$

At each time step, the equations of rigid body motion are solved if the object moves in a coupled fashion. Effects of hydraulic force (pressure and shear stress), gravitational force, non-inertial force and control force on coupled motion are considered. Control forces are extra forces and torques that can be applied to a moving object, for example, the engine thrust on a boat. Locations and orientations of all moving objects are tracked, and area and volume fractions are updated accordingly. Figure 1 illustrates how the volume and area fraction coefficients are computed in a two-dimensional rectangular mesh, as well as the source term on the right-hand side of Eq. (5). Within a control volume the solid boundary is approximated as a planar interface allowing for a simple evaluation of the unit normal and surface area for each such surface element. The FAVOR^{TM} method provides the means to impose accurate boundary conditions for fluid flow and heat transfer. Because of its high-order representation of the geometry, the total surface area and volume of a solid object approaches the exact value as the grid spacing is reduced.

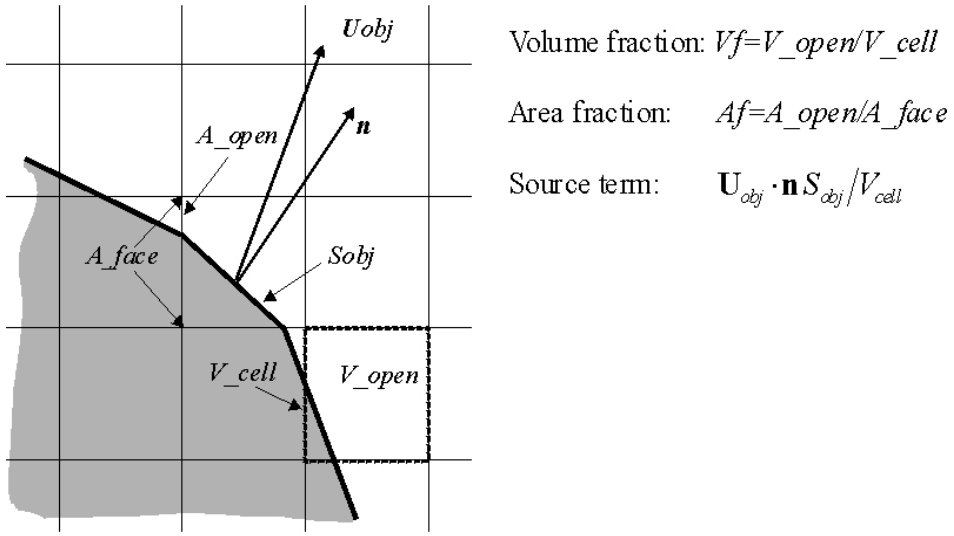

Figure 1. Schematic showing the calculation of area and volume fraction coefficients, A_f and V_f, for a solid object (shaded area) imbedded in a rectangular grid. The calculation of the source term for the continuity equation is shown for the central control volume.

Explicit approximations are used for the advective and viscous terms in the momentum equation, Eq. (6). The continuity equation, Eq. (4), is coupled with the momentum equation using the predictor-corrector method. An appropriate iteration scheme is then used to find the new pressure and velocity values [7].

Equation (7) is solved using a high-order interface tracking numerical scheme that employs geometric reconstruction of the interface to maintain accuracy during its advection [7, 8].

Results

The first test of the GMO model was done for a rectangular solid block of ice, 0.1 x 0.1 x 0.04 *m*, floating in a pool of water. The uniform density of the block was equal to 90 percent of the water density; therefore, at equilibrium only 90 percent of the block's volume should be submerged. The block was initially positioned horizontally, half-submerged in the water before being released under gravity at zero velocity into a quiescent pool of water. The block and water were initially at rest. The water was held by a cylindrical container 0.1 *m* deep and 0.2 *m* in diameter. Water pressure in the container was initialized to the hydrostatic distribution.

The motion of the block in water was modeled with the coupled six-DOF model. A three-dimensional uniform rectangular mesh was used with the grid spacing of 0.0035 *m*. Figure 2 shows the position of the ice block at selected times during the 10 seconds of simulation. After the release, the ice block bobs in the water, creating waves on the surface of the water. The waves in turn reflect off the walls of the container and further interact with the ice block. As a result, the block oscillates around its equilibrium position in all six degrees of freedom. The motion slowly dissipates due to viscous forces. Figure 3 shows the evolution of the vertical coordinate of its center of mass indicating that the solution is approaching equilibrium. The theoretical solution at z=-0.0117 *m* for the equilibrium position of the center of mass is also shown for comparison. If scaled by the vertical size of the ice block, the agreement between the equilibrium position estimated from the curve and the analytical solution is within a fraction of one percent.

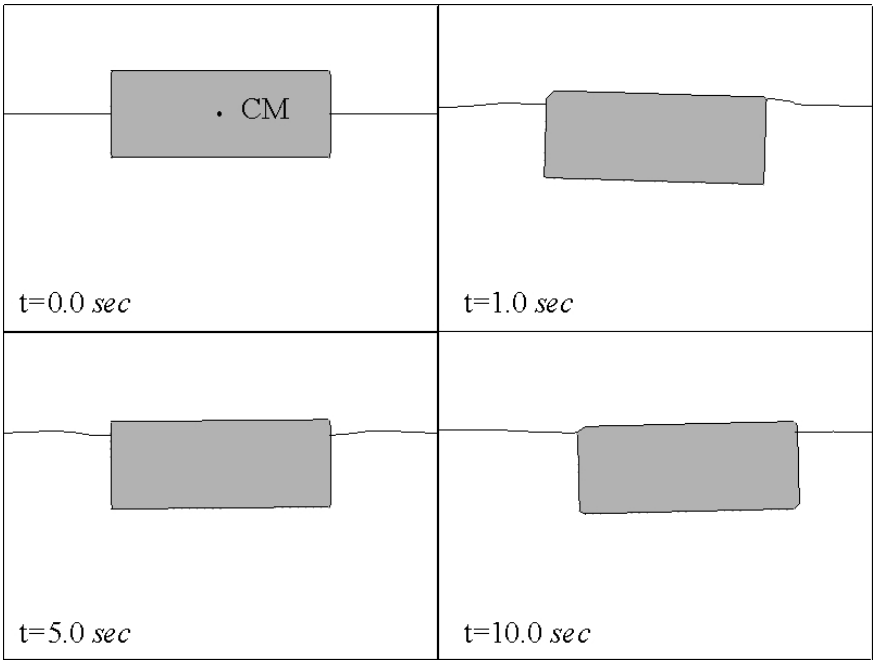

Figure 2. Position of the ice block (shaded area) and the shape of the free surface (shown in solid line) shown at selected times during the calculation. The images were obtained by making a vertical cross-section near the middle of the container. The location of the mass center is shown at t=0 *sec*.

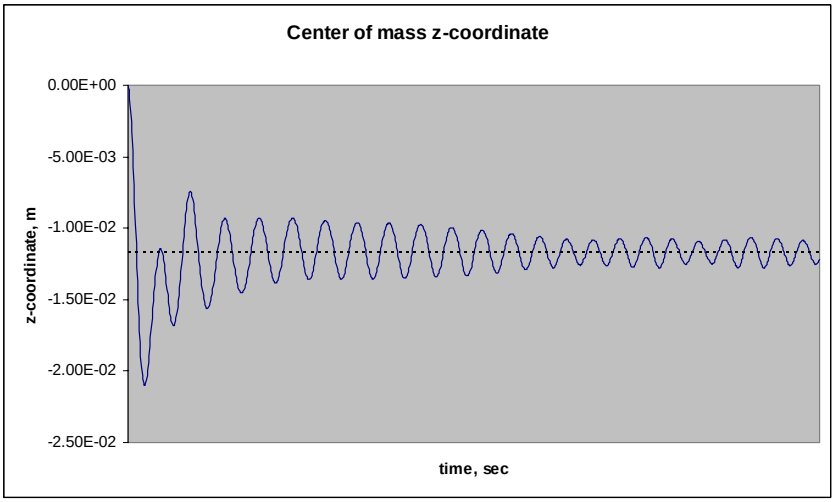

Figure 3. Evolution of the vertical coordinate of the mass center of the ice block after its release from the z = 0.0 (solid line). The analytical equilibrium solution at z=-0.0117 *m* is shown by the dashed line.

The second test involved a more dynamic interaction of a rigid body with water. An aluminum sphere, 0.099 *m* in diameter, was dropped vertically into a large quiescent pool of water with an initial speed of 8.8 *m/sec*. The projectile penetrates deep into the water, creating an air cavity in its wake as shown in Fig. 4 [9].

This process could be modeled by using a constant prescribed velocity of the sphere assuming it did not change significantly in the short time of the experiment, 0.15 *sec*, given the relatively large density of the sphere. However, we chose to use the fully coupled, six-DOF motion again. Additionally, pressure P within each air bubble created inside the pool was calculated as a function of the bubble's volume V, according to $(PV)^{\gamma} = const$, where γ=1.4 is the ratio of the specific heats for air. As in the previous case, the flow was modeled in a three-dimensional rectangular mesh with a uniform grid spacing of 0.006 *m*.

The results are shown in Fig. 4. The images in the simulation were chosen at the times when the penetration depth of the sphere approximately matched the three experimental images. The model predicts a somewhat smaller size of the upper cavity. The separation of the air cavity behind the sphere into two smaller cavities in the model occurs at a similar depth as in the experiment. The size and shape of the secondary air cavity right behind the sphere is also reasonably close to the experiment. The computed variation of the vertical component of the projectile's velocity shows that, despite the shortness of the time, it underwent a change of around 12% of the initial value. Therefore, the use of the coupled motion model was justified.

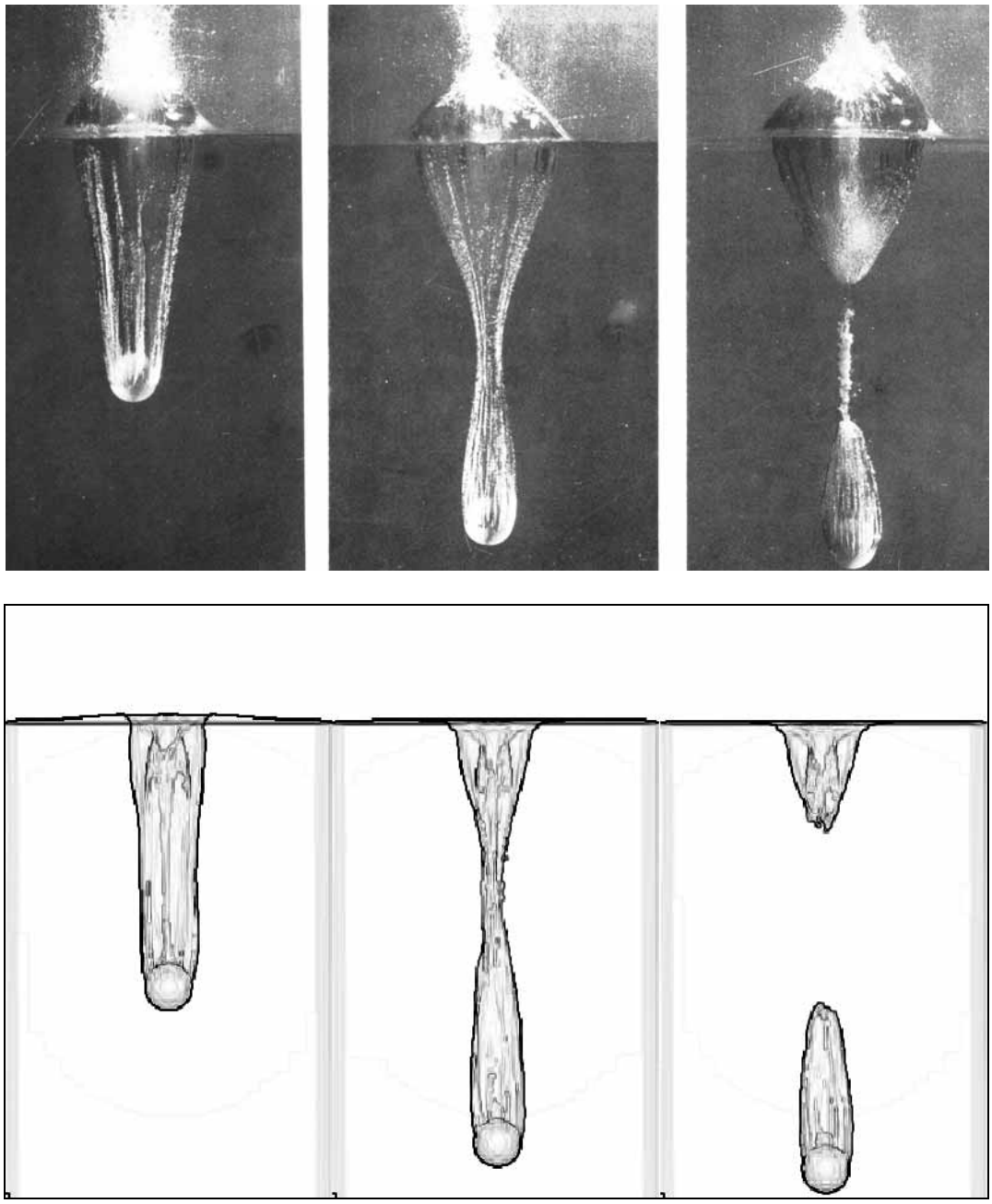

Figure 4. Cavity formed during entry of a sphere of diameter 0.099 *m* into water at a speed of 8.8 *m/sec*. Experimental results at the top were taken from [9]. The simulation images at the bottom show the bubble trail behind the sphere roughly at the same times as the experiment.

The final example employs the prescribed motion model, both translation and rotational, to simulate the process of pouring liquid metal from a ladle into a sand mold. The metal is initially placed into a vertically oriented ladle which then moves horizontally to a location above the pouring basin and stops. After stopping the ladle tilts forward 60 degrees, then recovers and moves back to the initial position – all in the time span of 10 seconds. The results of the simulation are shown in Fig. 5. There are no quantitative measurements to compare with, but the numerical results look reasonable. In addition to predicting realistic flow patterns, the total metal volume is conserved to less than 0.5% of the initial volume.

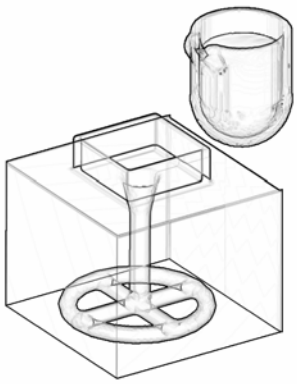

t=2.0 *sec*

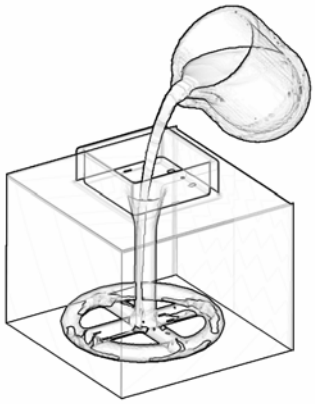

t=3.0 *sec*

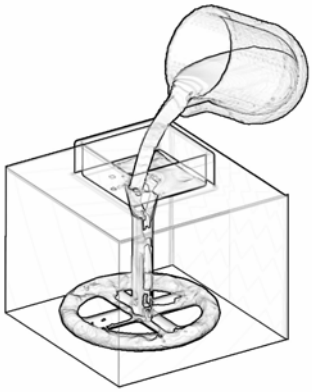

t=4.5 *sec*

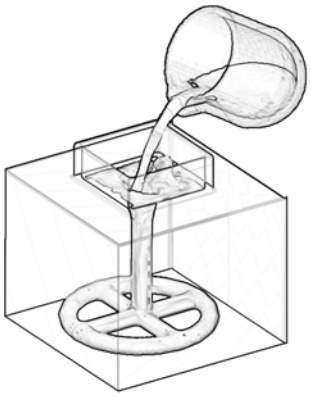

t=5.5 *sec*

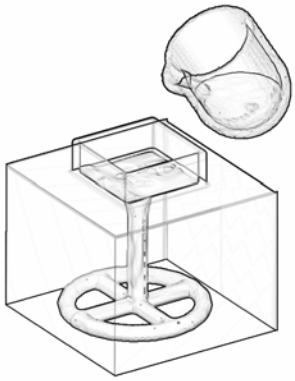

t=6.5 *sec*

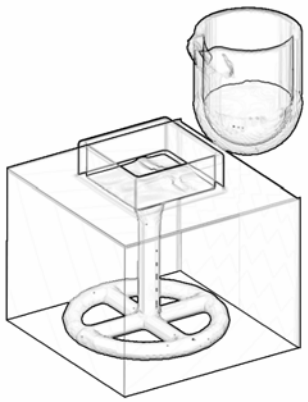

t=7.5 *sec*

Figure 5. The simulated pouring sequence of a liquid aluminum alloy from a ladle into a sand mold using the prescribed-motion GMO model. Images show only the rotational part of the ladle motion.

Conclusions

A fixed-mesh model for general moving objects (GMO) in a fluid has been developed and implemented into the commercial general-purpose CFD package ***FLOW-3D***® [10]. It allows multiple moving objects with different types of motion that are either prescribed or dynamically coupled with fluid flow. The use of fractional area and volume fractions to represent solid geometry in rectangular grids allows for an efficient way to model general motions of complex shapes.

The model yields good results for a floating ice block. The results of the model are also in reasonable agreement with the experimental images for a high-speed projectile impacting on a water surface. In general, the GMO model is applicable to a wide range of casting and other engineering processes that involve moving bodies such as pouring operations from ladles and furnaces, shot sleeves in high-pressure die casting and liquid and semi-solid forging.

References

1. J. Crank, *Free and Moving Boundary Problems* (Oxford, Oxford University Press, 1984).

2. B. A. Finlayson, *Numerical Methods for Problems with Moving Fronts* (Ravenna Park, WA, Ravenna Park Publishing, 1992).

3. C. W. Hirt and J. M. Sicilian, "A Porosity Technique for the Definition of Obstacles in Rectangular Cell Meshes", *Proc. Fourth International Conf. Ship Hydro.*, National Academic of Science, Washington, DC, Sept. 1985.

4. G. Wei, "A General Moving Object Model", (Technical Report TN-73, Flow Science Inc., 2005).

5. G. Wei, "A Fixed-Mesh Method for General Moving Objects in Fluid Flow," (Paper presented at the International Symposium on Physics of Fluids, Shuangshan, China, 5 June, 2005 and also submitted for publication in *Modern Physics Letters B, Special Issue on International Symposium on Physics of Fluids*, 19).

6. H. Goldstein, P. Charles and J. Safko, *Classical Mechanics* (Boston, MA, Addison Wesley and Company, 2002).

7. ***FLOW-3D***® Theory Manual, (Flow Science Inc., 2005).

8. C. W. Hirt and B. D. Nichols, "Volume of Fluid (VOF) Method for the Dynamics of Free Boundaries," *J. Computational Physics*, 39 (1981), 201-225.

9. G. K. Batchelor, *An Introduction to Fluid Dynamics*, (Cambridge, Cambridge University Press, 1983), 364, 365.

10. Flow Science, Santa Fe, New Mexico, USA, www.flow3d.com.